ELSEVIER

Polymer 44 (2003) 2149–2157

polymer

www.elsevier.com/locate/polymer

New performance of a modified poly(amide-12-*b*-ethyleneoxide)

A. Gugliuzza[a,*], E. Drioli[a,b]

[a]*Research Institute on Membrane Technology, ITM-CNR, Via Pietro Bucci 17/C, I-87030 Rende, Italy*
[b]*Department of Chemical Engineering and Materials, University of Calabria, Via Pietro Bucci 17/C, I-87030 Rende, Italy*

Accepted 10 January 2003

Abstract

The purpose of this work was the investigation of the water vapour transport through thermoplastic dense films of a poly(amide-12-*b*-ethylenoxide) such as Pebax®2533. Similar polymers have gained a unique position in many technologies for different reasons, such as their good physical properties, high processability, notable strength and transport properties to gases and vapours. Moreover, a rising demand of materials with specific characteristics in terms of water vapour transport comes from various market niches (i.e. textiles, building trade, packaging). For these reasons in this work particular attention has been paid to an elastomeric polymer such as the Pebax®2533, an easily processable material with good transport properties. Previous studies have pointed out that Pebax® copolymers can be used as precursors of membranes for separation processes of condensable vapours and gases. In this work a further investigation of the water transport properties through Pebax®2533 and derivative films allowed an understanding of their potential applications. The efficiency of these films has been tested by means of vapour permeability, solubility, diffusivity, and hydrophobicity/hydrophilicity measurements.

Keywords: Water vapour; Pebax; Membrane

1. Introduction

The water vapour transport through porous and dense films is of great interest for different industrial fields ranging from textile [1–3] to pharmaceutical [4,5], building trade [6] and dehydration process of gas streams [7,8]. In the last decades a lot of attention has been paid to the influence of chemical structure on gas [9–12] and vapour [13–15] transport through dense polymer films. The attempt to find a relationship between the polymer structure and the water vapour transport through polymeric membranes has been the goal of many works [14–17] in order to understand and plan the influence of chemical functionality and structure flexibility on the permeant species transport. Previous studies [18–20] have been focused on the use of additives in order to modify the physico-chemical properties of trade polymers. In this work the main interests were the attempt to improve, by means of addition of different organic compounds, the performance of a trade polymer such as the Pebax®2533, and the understanding of the vapour permeation mechanism, influence of temperature, component hydrophilicity and additive concentration in this system. Pebax®2533 shows the typical characteristics of an elastomeric polymer. It consists of a regular linear chain of rigid polyamide (Nylon 12, 20 wt%) interspaced with flexible polyether (PTMO). The amide blocks produce hard segments and the polyether blocks behave as soft segments. The main contribution to crystallinity of the copolymer comes from the amide block in which the less permeable phase resides, whereas the ether block acts as permeable phase for its high chain mobility. The vapour transport through dense Pebax®2533 films obeys to the solution-diffusion mechanism. The solubility into the polymer matrix depends on the favourable chemical interactions between permeant and polar chemical groups of the polymer, whereas the diffusivity is strictly connected to the mobility of the polymer chain, low packing density and hence the presence of microcavities with sufficient dimension to allow the passage of the vapour molecules. When adding organic molecules with different chemical structure to a polymer matrix, the system morphology, the chemical composition and even the physico-chemical properties change, influencing the transport through the

Abbreviations: TEC, triethylcitrate; KET, *N*-ethyl-*o*,*p*-toluene-sulphonamide; SB, sucrose benzoate.

* Corresponding author. Tel.: +39-984-492014; fax: +39-984-402103.
E-mail address: a.gugliuzza@itm.cnr.it (A. Gugliuzza).

0032-3861/03/$ - see front matter © 2003 Elsevier Science Ltd. All rights reserved.
doi:10.1016/S0032-3861(03)00037-5

Nomenclature

A	membrane area (cm^2)
a_w	water vapour activity (–)
C_1	the solubility of the permeant in the film at interface feed-membrane surface, respectively ($g\ cm^{-3}$)
D	diffusion coefficient of permeant ($cm^2\ s^{-1}$)
$D_s, D_{1/2}$	diffusion coefficients determined from response time t_s, $t_{1/2}$ ($cm^2\ s^{-1}$)
E_p, E_d	activation energies of water in permeation and diffusion ($kJ\ mol^{-1}$)
J	flux at time t ($g\ cm^{-2}\ s^{-1}$)
J_s	flux at steady-state condition ($g\ cm^{-2}\ s^{-1}$)
l	membrane thickness (cm)
P	permeance through membrane (cm^3(STP)/(cm^2 s cm Hg) $\times 10^{-6}$)
p_h	upstream pressure (cm Hg)
p_l	downstream pressure (cm Hg)
$p_{p(t)}$	downstream pressure at t_t (cm Hg)
Q_t	permeating amount per unit area for a given period of time ($g\ cm^{-2}$)
R	gas constant ($kJ\ mol^{-1}\ K^{-1}$)
S	solubility coefficients ($cm^3\ cm_{pol}^{-3}\ cm\ Hg^{-1}$)
STP	standard temperature, pressure ($T = 273.15$ K, $P = 1$ atm)
T	operating absolute temperature (K)
t	operating time (s)
$t_s, t_{1/2}$	response time (s)
ΔH_s	heat of sorption ($kJ\ mol^{-1}$)
ΔP	transmembrane pressure (cm Hg)
V	permeate volume (cm^3)
W_f, W_0	final and initial weights (g)
Greek symbols	
γ^-	base component of the surface free energy ($mN\ m^{-1}$)

membranes. Moreover, changes in mechanical characteristics also are expected. This work was only limited to the understanding of the transport phenomena; we need to underline, however, that the elastic behaviour of the films is preserved when adding triethylcitrate (TEC) and *N*-ethyl-*o*,*p*-toluenesulphonamide (KET) to the polymer solution, whereas a progressive stiffness of the materials appears for films ranging in sucrose benzoate (SB) concentration from 30 to 70 wt%.

The use of these species with relative low molecular weight allows reaching results similar to those obtained by hydrophilic/hydrophobic polymer blending, without inducing macroscopic phase separations.

2. Experimental

2.1. Materials

Pebax®2533 membranes were received from Procter & Gamble as dense films coated onto siliconized paper. These films were obtained by casting of polymer solutions and subsequent evaporation of the solvent mixture. Different organic molecules ranging in concentration from 30 to 70% (w/w) were added to polymer solutions. The organic compounds were triethylcitrate (TEC), *N*-ethyl-*o*,*p*-toluenesulphonamide (KET), sucrose benzoate (SB), whereas the solvents were toluene/2-propanol 50/50 v/v%.

2.2. Analytical methods

Water vapour permeability through films removed from the siliconized paper was measured at different temperatures by using gravimetric and flux transient techniques, respectively. The gravimetric experiments were performed according to cup method [21], and the flux transient tests with an apparatus for measuring gas and vapour permeability. The diffusion coefficients through the membranes were evaluated from permeation transients [22] and the solubility coefficients were derived from the ratio of the permeability and diffusion coefficient values according to $P = DS$ transport model [23]. The film thickness was measured using a digital gauge (Carl Mhar D 7300 Esslingen a. N.) for an average of 10 measurements with a deviation of ± 1.5 μm. Functional groups of dry thin films were investigated by FT-IR analysis in the transmission mode from 4000 to 400 cm^{-1}, with a resolution of 4 cm^{-1} and 10 scans (FT-IR Paragon 1330, Perkin Elmer). The base (electron donor) parameter γ^- ($mN\ m^{-1}$) of the surface free energy was estimated for each sample by sessile drop method at 20 °C using a CAM 200 contact angle meter (KSV instrument LTD, Helsinki, Finland). This method

consists in depositing the liquid probe by using an automatic microsyringe on the membrane surface. The three reference liquids were ultra pure water, glycerol and diiodomethane and the base γ^- component was calculated according to the Good, van Oss and Chaudhury method [24]. The T_g values for samples with 50 w/w% of additive were evaluated by dynamic mechanical thermal analysis (DMTA) of Polymer Laboratories MK 2, at 1 Hz, 3 °C min^{-1}, with strain 16 μm, ranging in temperature from −120 to +100 °C.

2.3. Permeability measurements

The following isothermal relation defines the water vapour permeability through the polymer membranes

$$P = J_s \frac{l}{p_h - p_l} \quad (1)$$

where J_s is the steady state rate of the vapour permeation through the unit area of thickness l when the p_h is upstream (high pressure) and p_l is the downstream pressure (low pressure), respectively. According to the gravimetric method, a cup was filled with distilled water and covered by dense film. After conditioning of 2 h the cup was put inside a thermostated dessicator with a drying agent in order to guarantee a constant driving force through the film cross-section, during the experiment. From the weight loss with time the permeation rate, expressed as permeance, was calculated at different operating temperatures according to the following relation

$$P = 22.414 \frac{(W_f - W_0)}{18AtΔP} \quad (2)$$

where W_f and W_0 are the final and initial weight of the cup, respectively; 22.414 is the number of cm^3(STP) $gmol^{-1}$; 18 is the molecular weight of H_2O; A is the effective membrane area, t is the length of time of a measurement; ΔP is the transmembrane water vapour pressure at operating temperature. The permeance was expressed as GPU where GPU = [cm^3(STP)/(cm^2 s cm Hg)] × 10^{-6}. The permeability coefficient was obtained from permeance values multiplied by the membrane thickness, expressed in cm. The thickness ranged from 20 to 40 μm. When the permeation transient experiments were performed, each membrane was put into a flat cell and dried under vacuum. The apparatus used for measuring permeability was thermostated at a fixed operating temperature. The upstream side of the membrane was in contact with a feed vessel at a constant water vapour activity ($a_w = 0.9$) for each temperature, whereas on the downstream side the pressure was negligible; in this way a constant driving force of the process was guaranteed. These experiments were performed measuring the pressure increase on the permeate side with time, according to the following relationship

$$P = \frac{V22.414}{RTAt} \ln\left(\frac{p_h - p_l}{p_h - p_{p(t)}}\right) \quad (3)$$

where V is the permeate volume (cm^3), R is the gas constant (8.31 kJ mol^{-1} K^{-1}) and T is the absolute temperature (K), A the membrane area (cm^2), t the measured time (s), p_h and $p_{p(t)}$ the downstream pressures at t_0 and t_t, respectively, and p_h the upstream pressure (cm Hg). The permeability coefficients were evaluated from the steady state values as shown in Fig. 1. Before each experiment the system and membranes were evacuated for some hours and in order to avoid condense phenomena the following procedure was applied:

- the upstream pressure was held slightly lower ($a_w = 0.9$) than the water vapour pressure at the operating temperature;
- the pressure rise in a fixed downstream volume was measured with time;
- on the downstream side the rising pressure range was selected narrow enough in order to keep the vapour activity close to zero [13], approaching the steady state;
- after each experiment the apparatus and films were flushed with N_2.

For each membrane the temperature of the permeation cell was changed from 20 to 35 °C and the effective membrane area was 2.14 cm^2.

2.4. Diffusion and solubility measurements

The diffusion behaviour of water vapour was derived from flux transients, evaluating two diffusion coefficients $D_{1/2}$ and D_{slope} at $t_{1/2}$ and t_{slope}, respectively. The $t_{1/2}$ is the time during which the flux rises from its initial value to one-half of its final value (i.e. steady state value), while the t_{slope} is the time between the onset and endset of the sigmoidal curve (Fig. 1). The two coefficients were derived from the following equations [25,26]

$$\frac{J}{J_s} = 1 + 2\sum_{n=1}^{\infty} \exp(n^2\pi^2 Dt/l^2) \quad (4)$$

where J and J_s are the fluxes in transient state and in steady state, respectively; l is the thickness of the membrane; D is the diffusion coefficient, and t is the permeation time. In a steady state permeation the amount of permeant Q_t, which passes through the film in time t, is equal to

$$Q_t = \frac{DC_1}{l}\left(t - \frac{l^2}{6D}\right) \quad (5)$$

and thus the flux J_s in a steady state becomes

$$J_s = \left(\frac{dQ_t}{dt}\right)_{t\to\infty} = \frac{DC_1}{l} \quad (6)$$

where C_1 is the solubility of the permeant in the film at interface feed-membrane. Combining Eqs. (4) and (6) the

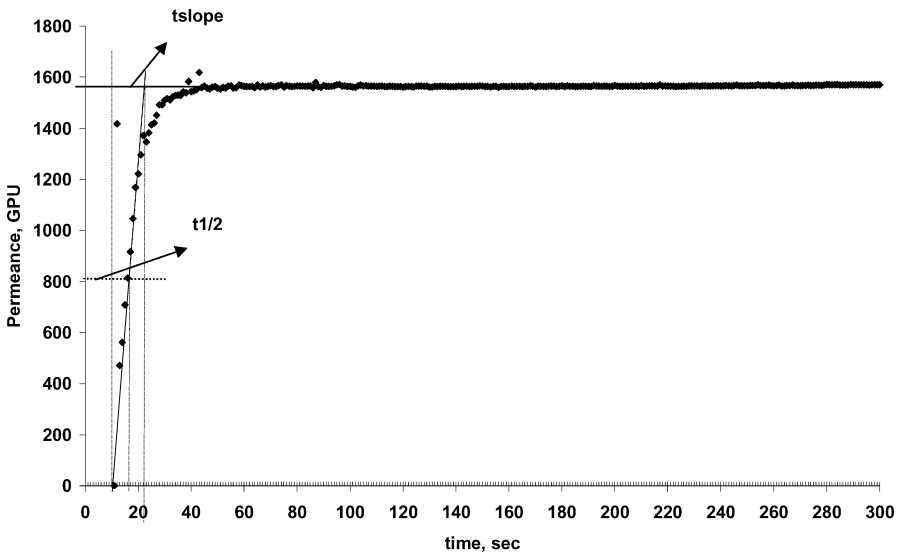

Fig. 1. Determination of response times from a transient gas flux transient through PEBAX® 2533 membranes at a given temperature.

flux can be rewritten as

$$J = \frac{\mathrm{d}Q_t}{\mathrm{d}t} = \frac{DC_1}{l}\left[1 + 2\sum_{n=1}^{\infty}(-1)^n \exp\left(\frac{-Dn^2\pi^2 t}{l^2}\right)\right] \quad (7)$$

and the two diffusion coefficients can be derived:

$$D_{1/2} = \frac{l^2}{7.2t_{1/2}} \quad (8)$$

$$D_s = \frac{l^2}{5.91t_s} \quad (9)$$

Solubility values were derived from permeability and diffusion coefficients according to solution-diffusion transport model $\bar{P} = \bar{D}\bar{S}$.

3. Results

The additives TEC, KET and SB were selected, in this order, for their decreasing hydrophilicity. All films, derived from Pebax®2533 and each of these additives at different concentrations, appeared to be homogeneous. There was no evidence of phase separation. Nevertheless, if membranes containing TEC are put in contact with other polymers, the additive tends to migrate towards the latter. In order to avoid this, the membranes must be stored between two siliconized paper sheets. The three additives are non-volatile. Additive loss was never observed during permeation experiments, as confirmed by FT-IR analysis before and after each experiment.

Water vapour permeance values obtained by both measurement methods were in a fair agreement. A permeance of 750 GPU, free example, was measured through pure Pebax®2533 at 27 °C by the cup method, while a value of 620 GPU was derived at 25 °C from permeation transient experiments. In this work only permeability values derived from latter method were reported according to Eq. (3). All experiments were performed at water vapour activity lower than unity in order to avoid both condense phenomena and phase separation induction [13]. A decrease in water vapour transport was observed changing from triethylcitrate (TEC) to sucrose benzoate (SB). A rising permeance through Pebax®2533 membranes was observed with increasing TEC content (Fig. 2), whereas a maximum was detected when KET was added at the 30 wt% (Fig. 3). An abrupt reduction of the permeance, lower than that of the pure polymer, was observed when the KET concentration increased to 70 wt% (Fig. 3). This reduction is even more evident in the case of SB, in particular at 70 wt%. In this case the breathability at 35 °C underwent a reduction of 90% with respect to the pure Pebax®2533 (Fig. 4). For all membranes the permeance increased with increasing temperature, obeying to the Arrhenius' law according to the following relationship:

$$P = P_0\, \mathrm{e}^{(-E_p/RT)} \quad (10)$$

In this equation E_p is the apparent activation energy for the

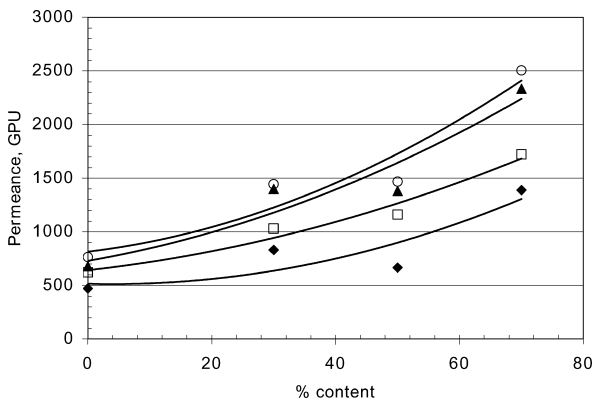

Fig. 2. Water vapour permeance versus TEC content: (◆) 20 °C, (□) 25 °C, (▲) 30 °C, (○) 35 °C.

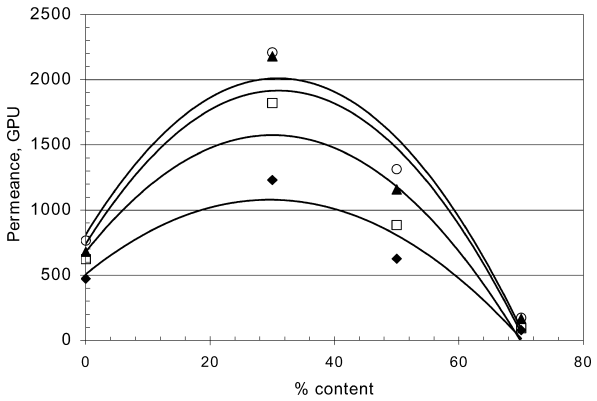

Fig. 3. Water vapour permeance versus KET content: (◆) 20 °C, (□) 25 °C, (▲) 30 °C, (○) 35 °C.

overall permeation processes (kJ mol^{-1}); P_0, is constant, R is the gas constant (8.31 kJ mol^{-1} K^{-1}) and T is the absolute temperature (K). The E_p values for all membranes are reported in Table 1. At high temperature the thermal motion of the polymer segments and the plasticisation action of the water vapour led to high permeant diffusion coefficients. The calculated diffusion coefficients D_s and $D_{1/2}$ were evaluated from $t_{1/2}$ and t_{slope} according to relationships described by Eqs. (8) and (9), respectively. The order of magnitude was on average 10^{-8} cm^2 s^{-1} for both coefficients, in agreement with the value reported for the pure polymer in the literature [16]. Both diffusion coefficients were plotted versus the temperature (Figs. 5–11) in Arrhenius mode and E_d was derived from the respective slopes (Table 1). In most cases both diffusion coefficients increased with increasing temperature. A slight increase in diffusion with respect to the pure polymer was observed through membranes with 30 wt% of additive; at higher additive concentration the diffusion coefficients decreased with increasing content of the additive. An exception was the Pebax/SB membrane, where the diffusion coefficients at 50 wt% were lower than those at 70 wt%. The diffusion process through these films required a lower activation energy at 70 wt%, as confirmed by the E_d values

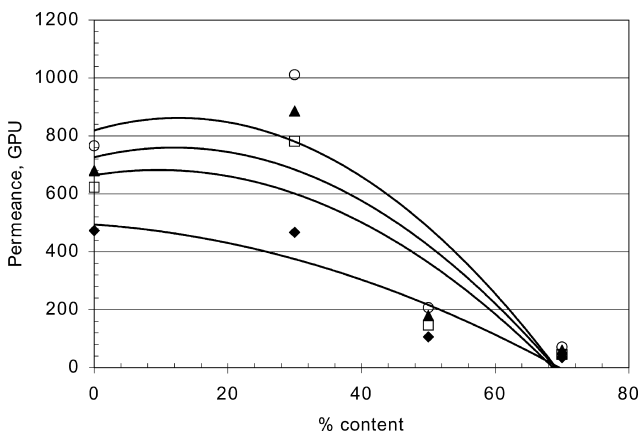

Fig. 4. Water vapour permeance versus SB content: (◆) 20 °C, (□) 25 °C, (▲) 30 °C, (○) 35 °C.

Table 1
The activation energies and heat of solutions of water determined from the flux transient at $a_w = 0.9$

Sample	w/w (%)	E_p (kJ mol^{-1})	E_d (kJ mol^{-1})	ΔH_s (kJ mol^{-1})
Pure Pebax	100/0	23.0	11.8	11.2
Pebax/TEC	70/30	13.5	13.4	0.07
Pebax/TEC	50/50	17.6	15.1	2.4
Pebax/TEC	30/70	14.3	23.2	−8.9
Pebax/KET	70/30	13.4	12.7	0.6
Pebax/KET	50/50	17.2	21.8	−4.6
Pebax/KET	30/70	20.5	20.8	−0.3
Pebax/SB	70/30	16.9	14.5	2.3
Pebax/SB	50/50	15.2	16.8	−1.6
Pebax/SB	30/70	17.1	10.5	6.5

reported in Table 1. Nevertheless, changing from TEC to SB, a reduction of the diffusion coefficients was observed. Generally, a difference between the two coefficients was detected. The diffusion calculated at $t_{1/2}$ was higher than that calculated at t_{slope}, confirming a non-ideal behaviour. The kinetic behaviour was conditioned by the physical property changes of the pure polymer as evidenced by results of the thermal analysis for samples with 50 wt%. TEC reduced the T_g while KET and Sucrose benzoate increased the glass transition temperature of the pure polymer (Table 2). Finally, the solubility values were derived from the following relationship:

$$S = \frac{P}{D_{slope}} \tag{11}$$

Changing the TEC concentration from 30 to 70 wt%, the solubility increased more than 70% (Table 2). When the KET was added to pure Pebax®2533, an increase in solubility was detected from 30 to 50% (w/w), while a sudden reduction was observed at 70 wt% (Table 2). In the polymer matrixes with sucrose benzoate the higher solubility value was measured at 50 wt% (Table 2). The favourable water vapour dissolution at this concentration

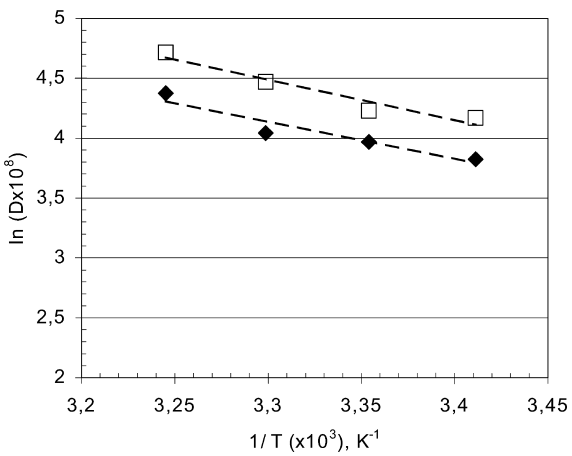

Fig. 5. Diffusion coefficients, (◆) D_{slope} and (□) $D_{1/2}$, through pure Pebax®2533 membrane according to Arrhenius' law.

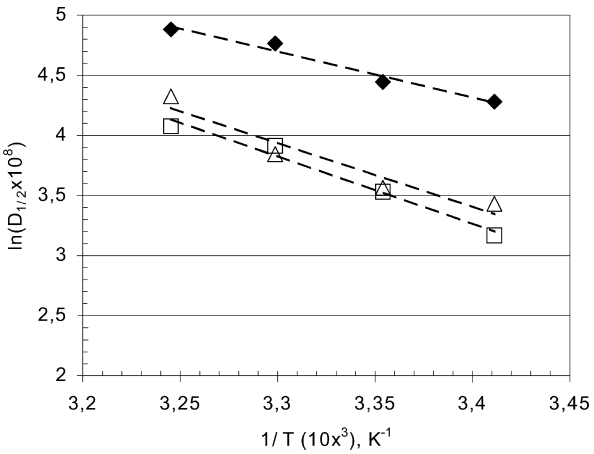

Fig. 6. Diffusion coefficients $D_{1/2}$ through Pebax/TEC membranes according to Arrhenius' law: (◆) 30 wt%, (△) 50 wt%, (□) 70 wt%.

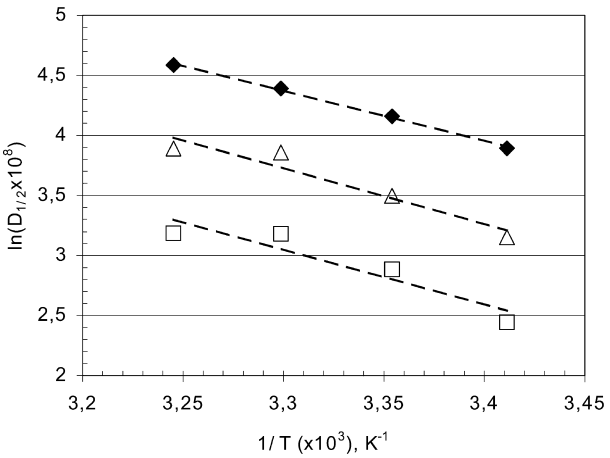

Fig. 8. Diffusion coefficients $D_{1/2}$ through Pebax/KET membranes according to Arrhenius' law: (◆) 30 wt%, (△) 50 wt%, (□) 70 wt%.

was confirmed by ΔH_s value (Table 1), derived from difference between E_p and E_d values.

A strong dependence of the solubility on the base component γ^- (mN m^{-1}) of the surface free energy (Table 2) was investigated as shown in Fig. 12. From a comparison of the membranes with additives at different polarity and at a parity of concentration, certain proportionality between surface hydrophilicity and solubility emerged. Similarly, this proportionality was detected between the permeance and base component of the surface free energy (Fig. 13).

4. Discussion

In the described experiments the breathability increased with increasing additive hydrophilicity, as observed for triethylcitrate (TEC), in contrast to what Schult and Paul [13] observed for polyethersulfone (PES) when adding polyethyloxazoline (PEOX). The latter, at 20 wt%, brought a remarkable decrease in diffusion coefficient as consequence of the free volume reduction. Differently, through Pebax films containing 70 wt% of a compound with low molecular weight such as TEC the decrease in diffusion coefficient at 35 °C equaled 56% versus the 93% detected through PES/PEOX 80/20 w/w%. This reduction was due to formation of hydrogen bonds between water molecules, citrate hydroxyl groups, and electron donor sites of the polymer segments, with consequent decrease in both the permeant mobility and chain mobility, as confirmed by FT-IR analysis shown in Fig. 14. The superposition of the relative Pebax/TEC spectra showed an increase in intensivity and widening of the typical hydroxyl band with increasing TEC concentration. Moreover, the O–H stretching bonds moved to lower frequencies, confirming the hydrogen bond formation. On the other hand, TEC could hinder the polymer segments from compacting themselves, with reduction of packing density and formation of microcavities through which the permeant moves itself, in particular at 30 wt% of TEC. Furthermore, the hydroxyl groups were also able to promote the water vapour dissolution into the polymer matrix, as confirmed by the increase in solubility at the concentration range of 30 to 70% (w/w) of additive. The influence of the solubility

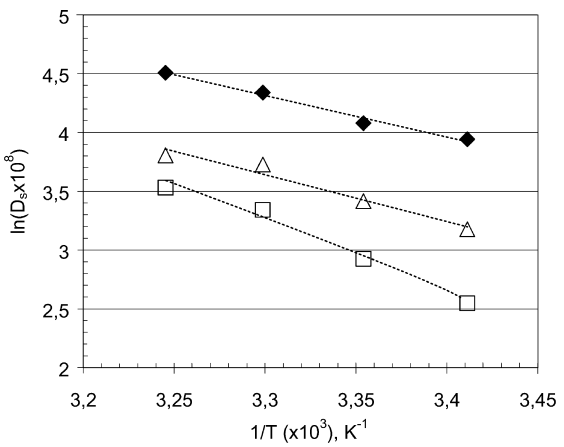

Fig. 7. Diffusion coefficients D_s through Pebax/TEC membranes according to Arrhenius' law: (◆) 30 wt%, (△) 50 wt%, (□) 70 wt%.

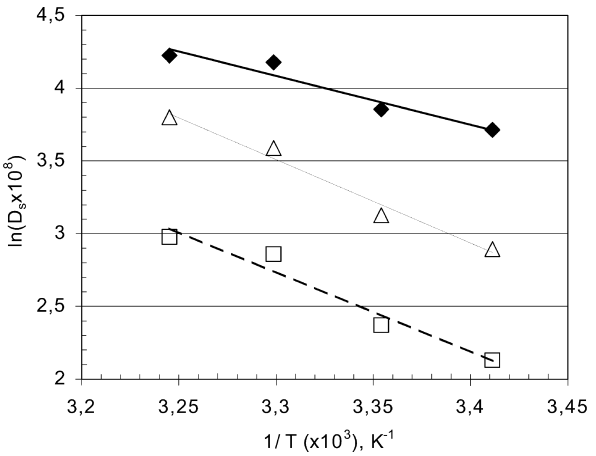

Fig. 9. Diffusion coefficients D_s through Pebax/KET membranes according to Arrhenius' law: (◆) 30 wt%, (△) 50 wt%, (□) 70 wt%.

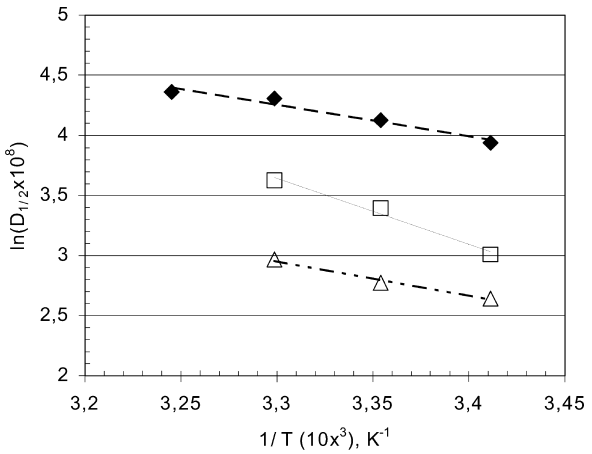

Fig. 10. Diffusion coefficients $D_{1/2}$ through Pebax/SB membranes according to Arrhenius' law: (◆) 30 wt%, (△) 50 wt%, (□) 70 wt%.

(thermodynamic parameter) was greater than the diffusivity (kinetic contribution), causing an overall increase in the water vapour permeability.

Differently, the rigid and sterically hindered aromatic structure of the KET and SB prevented the free rotation around the C–C bonds. The consequence was a stiff structure and a reduction of the probability of opening free volume transient gaps in which the permeant molecules could find allocation during their diffusion through the films. This effect was remarkable at additive contents above the 30 wt%.

The addition of organic compounds at 50 wt% gave rise to a permeability decrease. This was due to an influence of the kinetic contribution (D) larger than that of the thermodynamic parameter (S). Despite of the solubility for the membranes added at 50 wt% resulted always higher than that observed at 30 wt%, a reduction of the diffusion predominates on the solubility increase. This was also confirmed by the respective E_d values ranging from 30 to 50 wt%. When 70 wt% of KET was added, the permeability underwent a drastic reduction due to the considerably rigid

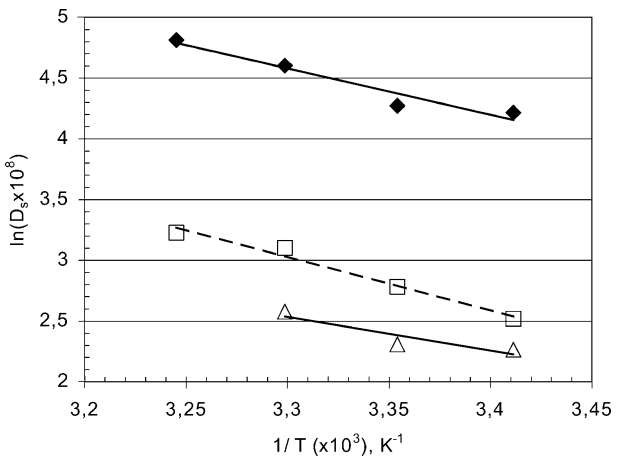

Fig. 11. Diffusion coefficients D_s through Pebax/SB membranes according to Arrhenius' law: (◆) 30 wt%, (△) 50 wt%, (□) 70 wt%.

Table 2
Base (electron donor) component of surface free energy calculated at 20 °C. T_g values related to the soft block of the Pebax®2533, and solubility coefficients calculated from 20 to 35 °C

Sample	w/w (%)	γ^- (mN m^{-1})	T_g (°C)	S (cm^3(STP)/cm$^3_{pol}$ cm Hg)			
				20 °C	25 °C	30 °C	35 °C
Pebax	100/0	9.8	−63	4.25	4.84	4.91	3.96
			−76 [16]				
Pebax/TEC	70/30	12.1		4.45	4.81	5.03	4.39
Pebax/TEC	50/50	28.0	−67	6.84	9.37	8.16	8.03
Pebax/TEC	30/70	32.3		21.76	18.47	16.50	14.66
Pebax/KET	70/30	12.1		6.17	7.93	6.87	6.65
Pebax/KET	50/50	19.9	−53	7.96	8.90	7.36	6.74
Pebax/KET	30/70	3.9		2.44	2.29	2.54	2.32
Pebax/SB	70/30	1.0		2.55	3.54	3.35	3.62
Pebax/SB	50/50	19.9	1	3.56	4.70	4.40	1.52
Pebax/SB	30/70	4.6		1.05	1.06	1.03	1.07

structure that decreased the mobility of the system. Moreover, at this content of additive the large weight of the hydrocarbon contribute with respect to polar groups such as sulphonamides restricted also favourable interactions with water vapour molecules. In the case of SB, a decrease in hydrophilicity was observed in all films. The reasons might be attributed to the masking of the sucrose hydroxyl groups as benzoate ester and the simultaneous increase in hydrocarbon component. Contact angle values higher than 80° confirmed a rising hydrophobicity of the film surface. At the interface feed-membrane the interactions between vapour and polymer matrix were limited with consequent decrease in solubility (Table 2). An exception in terms of diffusion was the film containing 70 wt% of SB. In fact, the energy for activating the diffusion process was lower than that measured for films containing 50 wt% of SB. Probably, the steric hindrance of the aromatic groups promoted an increase in free volume. Frozen gaps into polymer matrix facilitated the permeant passage through the film. However, since the decrease in solubility was greater than the increase in diffusion, the permeability decreased. The diffusion

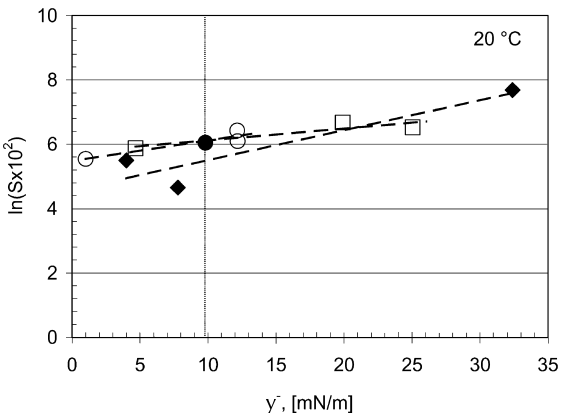

Fig. 12. ln S versus base component γ^- (mN m^{-1}) at 20 °C: (●) 0 wt%, (○) 30 wt%, (□) 50 wt%, (◆) 70 wt%.

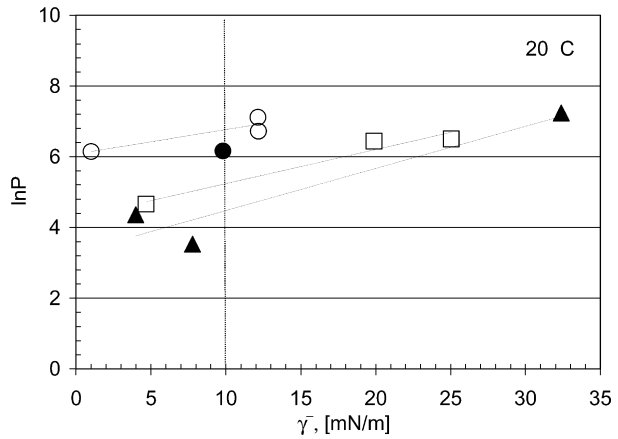

Fig. 13. ln P versus base component γ^- (mN m^{-1}) at 20 °C: (●) 0 wt%, (○) 30 wt%, (□) 50 wt%, (◆) 70 wt%.

process was activated by temperature and both coefficients, $D_{1/2}$ and D_s, increased with increasing temperature for all membranes. The non-ideality of the permeation transient was demonstrated by the difference between the two coefficients. The reason for this was the dependence of diffusion coefficient on the water vapour concentration from initiation to saturation of the permeation transients. Furthermore, the $D_{1/2}$ was higher than D_s for all samples at each temperature. The causes could be the following:

- when the additive is hydrophilic, e.g. triethylcitrate, the water dissolution is favoured, but the simultaneous hydrogen bond formation increases the permeant concentration in the polymer bulk, slowing down the diffusion during its permeation through the film;
- when the additive is sucrose benzoate, the hydrophobicity of the material promotes the cluster formation and the diffusion of water agglomerates becomes more difficult;
- if the added organic compound is the *N*-ethyl-*o*,*p*-toluenesulphonamide, both effects are evident and one predominates on the other one as a function of the additive content.

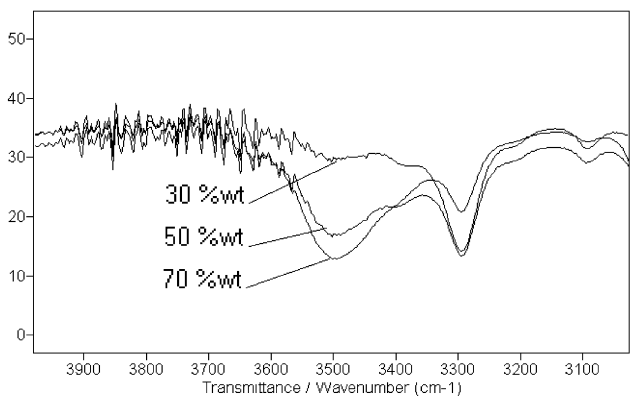

Fig. 14. FT-IR spectrum for Pebax/TEC films ranging in concentration from 30 to 70 wt%. Transmittance versus wavenumber (cm^{-1}).

The strict relationship between the chemical structure and diffusivity was emphasized by T_g of the soft segments of the block copolymer. In the Pebax/TEC 50/50 w/w% the glass transition was slightly lower than that of the pure Pebax. This points out a competition between two effects: the interaction of the TEC hydroxyl group with ether oxygen of the Pebax soft block promotes a reduction of the packing density, but simultaneously the hydrogen bonds do not allow large mobility of the polymer chains. Rigid and sterically hindrance aromatic structures such as those of KET and SB freeze the soft block of the polymer, promoting the formation of less permeable domains into polymer matrix. This was confirmed by the remarkable increase in the T_g values of the polymers containing KET and SB with respect to that of the pure Pebax (Table 1). Comparing the solubility and γ^- values the relation between high solubility and high hydrophilicity of the materials was emphasized. The electron donor γ^- (mN m^{-1}) is the base component of the surface free energy and so it can be considered an indirect indicator of the tendency to adsorb water on surface and to dissolve water at the interface feed-membrane. A high electron donor component means a high concentration of polar groups on the surface, able to interact favourably with a permeant such as water. The trends observed (Fig. 12) underline the large influence of surface solubility on total sorption. This means that the solubility is related to the material hydrophilicity and as consequence also the permeability becomes a function of the base component of the free energy, when different materials at a parity of concentration are compared. Nevertheless, the kinetic effects, bound to morphologic and structural aspects, cannot be neglected.

5. Conclusion

The addition of organic compounds with different physico-chemical properties allowed to change the performance of a traditional polymer such as the Pebax®2533. The water vapour permeability was influenced by the concentration and hydrophilicity of the additives. In the following the observed water vapour transport phenomena, through modified membranes based on Pebax®2533, are summarised:

1. The water vapour flux depends on the nature of the additives. TEC exalts the transport, while SB gives rise to a drastic reduction of the vapour passage through the membranes. KET increases or decreases the water vapour permeance, depending its concentration into polymer matrix. The permeance generally decreases with decreasing additive hydrophilicity, even if the process is activated by the temperature.
2. The diffusion also depends on both the temperature and concentration, respectively. With increasing temperature the diffusion tends to increase according to Arrhenius'

law, but at concentrations higher than 30 wt% of additive a reduction of the diffusion coefficient is observed. The reason for this is the immobilization of polymer chains due to the hydrogen bond formation or steric hindrance by aromatic structures.

3. The solubility is influenced by the hydrophilicity of the materials in a significant way, as confirmed by relationship between the solubility and base component γ^- of the surface free energy. The surface solubility contribution has a large weight on the total solubility. When adding polar organic compounds, the surface becomes more hydrophilic with respect to that of the pure polymer, promoting favourable interactions with water vapour at the interface feed-membrane.

The higher the surface hydrophilicity, the higher the permeance becomes. This is evident when correlating the water vapour transport through the membranes, containing different additives at a parity of concentration, to the base component γ^- of the surface free energy.

Acknowledgements

We acknowledge the contribution and financial support of PROCTER&GAMBLE-IRC (Italian Research Center-Pescara) to this work. The authors wish to thank Dr J. Jansen from ITM-CNR for his suggestions in the discussion of the results.

References

[1] Gugliuzza A, Clarizia G, Golemme G, Drioli E. New breathable and waterproof coatings for textiles: effect of an aliphatic polyurethane on the formation of PEEK-WC porous membranes. Eur Polym J 2002;38: 235–42.
[2] Elberaichi A, Daro A, David C. Water vapour transport in polyethylene oxide/polymethyl methacrylate blends. Eur Polym J 1999;35:1217–28.
[3] Gibson PW. Effect of temperature on water vapour transport through polymer membrane laminates. Polym Testing 2000;19:673–91.
[4] Corveleyn S, De Smedt S, Remon JP. Moisture absorption and desorption of different rubber lyophilisation closures. Int J Pharm 1997;159:57–65.
[5] Minghetti P, Cilurzo F, Liberti V, Montanari L. Dermal therapeutic systems permeable to water vapour. Int J Pharm 1997;15:165–72.
[6] Barbucci A, Delucchi M, Cerisola G. Organic coatings for concrete protection: liquid water and water vapour permeabilities. Prog Org Coat 1997;30:293–7.
[7] Scovazzo P, Hoehn A, Todd P. Membrane porosità and hydrophilic membrane-based dehumidification performance. J Membr Sci 2000; 167:217–25.
[8] Ito A. Dehumidification of air by a hygroscopic liquid membrane supported on surface of a hydrophobic microporous membrane. J Membr Sci 2000;175:35–42.
[9] Kim JH, Ha SY, Lee YM. Gas permeation of poly(amide-6-b-ethylene oxide) copolymer. J Membr Sci 2001;190:179–93.
[10] Pixton MR, Paul DR. Gas transport properties of polyarylates part I: connector and pendant group effects. J Polym Sci, Part B: Polym Phys 1995;33:1135–49.
[11] Pixton MR, Paul DR. Gas transport properties of polyarylates part II: tetrabromination of the bisphenol. J Polym Sci, Part B: Polym Phys 1995;33:1353–64.
[12] Bondar VI, Freeman BD, Pinnau I. Gas transport properties of poly(ether-b-amide) segmented block copolymers. J Polym Sci, Part B: Polym Phys 2000;38:2051–62.
[13] Schult KA, Paul DR. Water sorption and transport in a series of polysulfones. J Polym Sci, Part B: Polym Phys 1996;34:2805–17.
[14] Kelkar AJ, Paul DR. Water vapour transport in a series of polyarylates. J Membr Sci 2001;181:199–212.
[15] Shigetomi T, Tsuzumi H, Toi K, Ito T. Sorption and diffusion of water vapour in poly(ethylene terephthalate) film. J Appl Polym Sci 2000; 76:67–74.
[16] Rezac ME, Tilo J. Correlation of permeant transport with polymer free volume: additional evidence from block copolymers. Polymer 1998;39:599–603.
[17] Lokhandwala KA, Nadakatti SM, Stern SA. Solubility and transport of water vapour in some 6FDA-based polyimides. J Polym Sci, Part B: Polym Phys 1995;33:965–76.
[18] WO 99640077.
[19] WO 9964505.
[20] WO 9964078.
[21] 4818 UNI part 26 procedure.
[22] Yeom CK, Kim BS, Lee JM. Precise on-line measurements of permeation transients through dense polymeric membranes using a new permeation apparatus. J Membr Sci 1999;161:55–66.
[23] Noegi P. Diffusion in polymers. NY: D. Dekker Press; 1996.
[24] Good RJ, Van Oss CJ. In: Schroder ME, Loeb GL, editors. Modern approaches to wettability. NY: Plenum Press; 1992.
[25] Watson JM, Payne PA. A study of organic compound pervapouration through silicon rubber. J Membr Sci 1990;49:171.
[26] Watson JM, Baron MG. Precise static and dynamic permeation measurement using a continuous-flow vacuum cell. J Membr Sci 1995;106:259.